CHAPTER 12

Analysis of Polysaccharide Size, Shape and Interactions

STEPHEN E. HARDING

1 Introduction

In the earlier Royal Society of Chemistry book *Analytical Ultracentrifugation in Biochemistry and Polymer Science*, we reviewed the progress and potential of the ultracentrifuge for providing fundamental information about polysaccharides in what for many is their natural state – in solution.[1] Our chapter was reinforced by contributions from Lavrenko and co-workers,[2] who looked in detail at the concentration dependence of the sedimentation coefficient of polysaccharides, Comper and Zamparo,[3] who reviewed the sedimentation analysis of proteoglycans, and Preston and Wik,[4] who examined the non-ideality behaviour of hyaluronan. Since the publication of that book, there has been the launch and establishment of the XL-I analytical ultracentrifuge with full on-line data automatic data capture analysis, concurrent with a general phasing out of the older MOM 2081, MSE Centriscan and Beckman Model E analytical ultracentrifuges, although the latter facilitated off-line automatic data capture and analysis.[5,6]

These developments have facilitated some major advances in software for analysis. Although the focus of these advances has been for the study of protein systems, they also, with some adjustment where appropriate, present possibilities for the study of polysaccharides and related glycopolymers. And alongside these developments in instrumentation and analysis software, there have been some important developments with related techniques such as size-exclusion chromatography and atomic force microscopy. This chapter reflects on these advances and considers how the new generation of analytical ultracentrifugation is contributing, where appropriate in combination with other techniques, to our understanding of the size, shape and interactions of polysaccharides in a solution environment. It will also reflect on some of the special difficulties they still present compared to the study of protein systems, most notably deriving from their polydispersity and non-ideality.

2 Change in Instrumentation

Although a handful of Beckman Model E and MOM ultracentrifuges remain in use, since its launch in 1996 the principal analytical ultracentrifuge used for the

study of polysaccharide solutions has become the Optima XL-I from Beckman Instruments (Palo Alto, USA).[7] Six years earlier, the Beckman Optima XL-A ultracentrifuge had been launched with online UV/visible absorption optics providing a direct record of solute concentration (in absorption units) $c(r)$ *vs.* radial displacement r from the axis of rotation.[8] This optical system however had limited relevance for polysaccharides because of the lack of chromophore these substances possess in the near-UV (250–300 nm) and visible region. Nonetheless, some studies on labelled polysaccharides were possible and Cölfen and co-workers in 1996[9] successfully used an XL-A to characterise the sedimentation coefficient and molecular weight of two chitosans labelled with the fluorophore 9-anthraldehyde.

The laser (wavelength 670 nm) on the XL-I instrument provides high-intensity, highly collimated light and the resulting interference patterns (between light passing through the solution sector and reference solvent sector of an ultracentrifuge cell) are captured by a CCD camera. A Fourier transformation converts the interference fringes into a record of concentration $c(r)-c(a)$ relative to the meniscus ($r=a$) as a function of r. The measurement is in terms of Rayleigh fringe units relative to the meniscus, $j(r)$, with $J(r)=j(r)+J(a)$, $J(r)$, being the absolute fringe displacement and $J(a)$ the absolute fringe displacement at the meniscus. For a standard optical path length cell ($l=1.2$ cm) with laser wavelength $\lambda=6.70\times10^{-5}$ cm, a simple conversion exists from $J(r)$ in fringe displacement units to $c(r)$ in g mL^{-1}:

$$c(r) = \frac{J(r)\lambda}{(\mathrm{d}n/\mathrm{d}c)l} \qquad (1)$$

$$= \left\{\frac{5.58\times10^{-5}}{(\mathrm{d}n/\mathrm{d}c)}\right\}\cdot J(r)$$

with similar conversions for $J(a)$ to $c(a)$ and $j(r)$ to $c(r)-c(a)$. dn/dc is the (specific) refractive index increment, which depends on the polysaccharide, solvent and wavelength. A comprehensive list of values for a range of macromolecules has recently been published.[10] In aqueous systems, most values lie between 0.14 and 0.16 mL g^{-1}, although for non-aqueous systems the values can range enormously from 0.044 to 0.218 mL g^{-1}. The data, for example, for κ-carrageenan suggest little temperature dependence although that for dextrans suggests a significant dependence on wavelength. A study on the polycationic chitosan[11] suggested that the degree of substitution of some polysaccharides can strongly affect dn/dc, particularly if ionic groups are involved. Preston and Wik[4] have explored in detail the effect of ionic strength and wavelength on dn/dc for the polyanion hyaluronate. These results show that if a user needs, for whatever reason, an accurate value for dn/dc for a polysaccharide, he should measure it directly in the particular buffer used for the ultracentrifuge experiments. Converting fringe concentrations {$j(r)$ or $J(r)$} into weight concentrations is normally not necessary for most applications. In addition, for sedimentation velocity work it is possible to work with $j(r)$ or $c(r)-c(a)$, *i.e.* concentrations relative to the meniscus without having to worry about measuring the offset or meniscus concentration $J(a)$ or $c(a)$ to convert into absolute $J(r)$ or $c(r)$.

3 Polysaccharide Polydispersity and Simple Shape Analysis by Sedimentation Velocity

Traditional analysis methods on optical records from sedimentation velocity experiments have been based around recording the movement of the radial position of the boundary r_b with time t, from which a sedimentation coefficient, s (s or Svedbergs, S, where 1 S$=10^{-13}$ s) can be obtained:[12]

$$s = \frac{(dr_b/dt)}{\omega^2 r_b} \tag{2}$$

Where ω is the angular velocity (rad s^{-1}) and followed by the usual correction to standard conditions – namely the density and viscosity of water at 20.0 °C – to yield $s_{20,w}$[12] and the algorithm SEDNTERP, which also arose out of the 1992 volume[13,14] has been useful facilitating this correction. Non-ideality effects are much more severe for polysaccharides compared with proteins, and the traditional way of correcting for such non-ideality is to measure either s or $s_{20,w}$ for a range of different cell loading concentrations c, and perform an extrapolation to zero concentration. For polysaccharides, this has been conventionally achieved from a plot of $1/s$ (or $1/s_{20,w}$) *vs.* c:[12]

$$\{1/s\} = \{1/s^\circ\}\cdot\{1 + k_s c)\} \tag{3}$$

a relation valid over a limited range of concentration with k_s the Gralén coefficient named after his doctoral dissertation on the analysis of cellulose and its derivatives.[15]

For a wider span of concentrations, a more comprehensive description of concentration dependence has been proposed by Rowe:[16,17]

$$s = s^\circ\left\{1-\frac{\left[k_s c-\left(\frac{(c\nu_s)^2(2\phi_p-1)}{\phi_p^2}\right)\right]}{[k_s c-2c\nu_s+1]}\right\} \tag{4}$$

Where ν_s (mL g^{-1}) is the 'swollen' specific volume of the solute (volume (mL) of a polysaccharide (swollen through solvent association) per gram of the anhydrous molecule) and ϕ_p is the maximum packing fraction of the solute (~0.4 for biological solutes.[17]) A least-squares proFit (Quantum Soft, Zurich, Switzerland) algorithm has been developed for fitting s *vs.* c data to Equation (4), and as we will see below, this relation is proving to be of interest for the analysis of polysaccharides.

3.1 Sedimentation Coefficient Distributions: SEDFIT

The ability to acquire multiple data on-line with the XL-A and XL-I has formed the catalysis for advances in software for recording and analysing not only the change in boundary position with time but the change in the whole radial concentration profile, $c(r, t)$ with time t. These advances have in particular facilitated the measurement of *distributions* of sedimentation coefficient.[18–22] The (differential) distribution of

sedimentation coefficients can be defined as the population (weight fraction) of species with a sedimentation coefficient between s and s+ds. Different symbols exist for this parameter, either $g(s)$ or $c(s)$: despite the choice of symbol for the latter, unlike c and $c(r,t)$, $c(s)$ has units of weight concentration (g mL^{-1}) *per second or Svedberg unit*. A plot of $g(s)$ or $c(s)$ *vs.* s then defines the distribution. Integration of a peak or resolved peaks from these types of plot can then be used to calculate the weight average s of the sedimenting species and their partial loading concentrations.

The simplest way of computationally obtaining a sedimentation coefficient distribution is from time derivative analysis of the evolving concentration distribution profile across the cell.[18,19] More recently, attention has turned to direct modelling of the evolution of the concentration distribution with time for obtaining the sedimentation coefficient distribution.[20,21] The distribution has been related to the experimentally measured evolution of the concentration profiles throughout the cell by a Fredholm integral equation

$$a(r, t) = \int_{s_{min}}^{s_{max}} c(s)\cdot\chi(s, D, r, t)\, \mathrm{d}s + a_{TI}(r) + a_{RI}(t) + \varepsilon \qquad (5)$$

In this relation, $a(r, t)$ is the experimentally observed signal, ε represents random noise, $a_{TI}(r)$ the time-invariant systematic noise and $a_{RI}(t)$ the radial-invariant systematic noise. Schuck[20] and Dam, and Schuck[21] describe how this systematic noise is eliminated. χ is the normalised concentration at r and t for a given sedimenting species of sedimentation coefficient s and translational diffusion coefficient D: it is normalised to the initial loading concentration so it is dimensionless. The evolution with time of the concentration profile $\chi(s, D, r, t)$ for a given sedimenting species of sedimentation coefficient s and translational diffusion coefficient D in a sector-shaped ultracentrifuge cell is given by the Lamm[23] equation: although only approximate analytical solutions to this partial differential equation have been available for $\chi(s, D, r, t)$, accurate numerical solutions are now possible using finite element methods first introduced by Claverie and co-workers[24] and recently generalized to permit greater efficiency and stability.[20,21] The algorithm SEDFIT[25] employs this procedure for obtaining the sedimentation coefficient distribution. To solve Equation (5) to obtain $c(s)$ as a function of s requires the limits s_{min} and s_{max} to be carefully chosen and adjusted accordingly: inappropriate choice can be diagnosed by an increase of $c(s)$ towards the limits of s_{min} or s_{max}. However, the contribution from diffusion broadening also has to be dealt with. SEDFIT offers two ways. The first is using a dependence of D on s, via the translational frictional ratio f/f_0:

$$D(s) = \left\{\frac{\sqrt{2}}{18\pi}\right\} k_B t s^{-1/2} (\eta_o (f/f_0)_w)^{-3/2} \left(\frac{1-v\rho_o}{v}\right)^{-1/2} \qquad (6)$$

where f is the frictional coefficient of a species, f_0 the corresponding value for a spherical particle of the same mass and (anhydrous) volume (see *e.g.* ref. 26) and k_B is the Boltzmann constant. Although, of course, a distribution of s implies also a distribution in D and f/f_0, for protein work, advantage is taken of the fact that the frictional ratio is a relatively insensitive function of concentration: a single or weight average f/f_0 is taken to be representative of the distribution. Using this assumption, of Equation (5) can be numerically inverted to give the sedimentation coefficient distribution, with the position and shape of the $c(s)$ peak(s) more representative of a true distribution of sedimentation

coefficient. $(f/f_0)_w$, where the subscript w denotes a weight average, is determined iteratively by non-linear regression, optimizing the quality of the fit of the $c(s)$ as a function of $(f/f_0)_w$. It has been shown by extensive simulation that non-optimal values of $(f/f_0)_w$ have little effect on the position of the $c(s)$ peaks, although affects the width and resolution, *i.e.* the correct s value is reported. Regularization[25] can be used which provides a measure of the quality of fit from the data analysis. The assumption of a single f/f_0 representing the whole macromolecular distribution may be reasonable for proteins but it is open to question whether this is so for polysaccharides: this assumption will affect the reliability of distribution widths, but not peaks. Nonetheless, better approximations are currently being sought.

The present version of SEDFIT also offers the option of evaluating the distribution corresponding to non-diffusing particles, *viz* D~0, *i.e.* the diffusive contribution to Equation (5) is small compared to the sedimentation contribution. In this case, Equation (5) can be inverted without any assumptions concerning f/f_0. If diffusive effects are significant, it will lead to an apparent sedimentation coefficient distribution, given as $g^*(s)$ *vs.* s although the correct s value for a peak is still reported. Figure 1 gives a comparison of the least-squares $g^*(s)$ *vs.* s and $c(s)$ *vs.* s distribution for guar gum.[27]

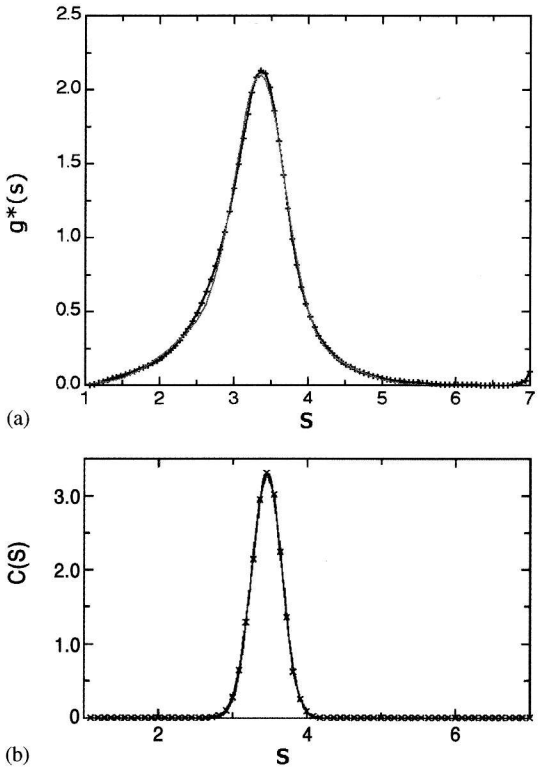

Figure 1 *Sedimentation concentration distribution plots for guar gum using SEDFIT. (a) g*(s) vs. s; (b) c(s) vs. s. A Gaussian fit to the data (lighter line) is also shown in (a). Rotor speed was 40 000 rpm at 20.0 °C, concentration was ~0.75 mg mL^{-1} in 0.02% NaN_3. The guar had been heated at 160 °C for 10 min at a pressure of 3 bar (from ref. 27)*

There is a clear shoulder on the low s (lower M) side of the $g^*(s)$ peak – consistent with some lower molecular weight material observed using the technique of SEC–MALLs (size-exclusion chromatrography coupled to multi-angle laser light scattering), whereas the $c(s)$ profile shows only a symmetric peak. The current $c(s)$ procedure in this instance seems to have 'oversmoothed' the data. We would suggest the evaluation of apparent distributions via $g^*(s)$ is preferred at present, particularly for slow-diffusing polysaccharides.

It is possible to get molecular weight from the sedimentation coefficient if we assume a conformation or if we combine with other measurements, namely the translational diffusion coefficient via the Svedberg equation[28]

$$M = RT\,\frac{\{s^\circ/D^\circ\}}{(1-\bar{\nu}\rho_o)} \tag{7}$$

where ρ_o is the solvent density (if s and D are their normalized values $s^\circ_{20,w}$, $D^\circ_{20,w}$, ρ_o will be the density of water at 20.0°C, 0.9981 g mL^{-1}). Equation (7) has been popularly used, for example, to investigate the molecular weights of carboxymethylchitins,[29–31] glycodendrimers,[32,33] β-glucans[34] and alginates.[35] The translational diffusion coefficient in Equation (7) can in principle be measured from boundary spreading as manifested, for example, in the width of the $g^*(s)$ profiles: although for monodisperse proteins, this works well, for polysaccharides, interpretation is seriously complicated by broadening through polydispersity. Instead, special cells can be used which allow for the formation of an artificial boundary whose diffusion can be recorded with time at low speed (~3000 rev per min). This procedure has been successfully employed, for example, in a recent study on heparin fractions.[36] Dynamic light scattering has been used as a popular alternative, and a good demonstration of how this can be performed to give reliable D data has been given by Burchard.[37]

Whereas the s° is a weight average, the value returned from dynamic light scattering for D° is a z average. As shown by Pusey,[38] combination of the two via the Svedberg equation (7) yields the weight-average molecular weight M_w, although it is not clear what type of average for M is returned if an estimate for D° is made from ultracentrifuge measurements.

Another useful combination that has been suggested is $s^\circ_{20,w}$ with k_s:[16,17]

$$M_w = N_A\left[\frac{6\pi\eta s^\circ_{20,w}}{(1-\bar{\nu}\rho_0)}\right]^{3/2}\left[\frac{3\bar{\nu}}{4\pi}\left(2\frac{k_s}{\bar{\nu}}\right)-\left(\frac{\nu_s}{\bar{\nu}}\right)\right]^{1/2} \tag{8}$$

s, k_s and ν_s can be obtained from fitting s *vs.* c data to Equation (4). The method was orginally developed for single solutes and where charge effects can be neglected (either because the macromolecular solute is uncharged, or because the double layer or polyelectrolyte behaviour has been 'compressed' by addition of neutral salt). For quasi-continuous distributions, such as polysaccharides, one can apply Equations (5) and (8) to the data, provided that for every concentration one has a 'boundary' to which a weight-averaged s value can be assigned. If the plot of $1/s$ *vs.* c is essentially linear over the data range, then specific interaction can be excluded, the solute system treated as a simple mixture and Equations (5) and (8) can be applied. Figure 2 shows an example for wheat starch amylopectin, where concentrations for total

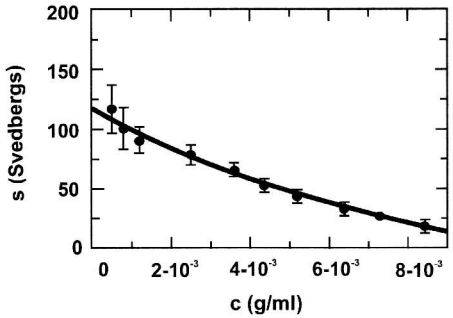

Figure 2 *Concentration dependence of the sedimentation coefficient for wheat amylopectin. The data have been fitted to Equation (4) (see text) yielding* $s°=(120\pm10)$ *S,* $k_s=(170\pm60)$ *mL* g^{-1} *and* $v_s=(40\pm4)$ *mL* g^{-1} *(from ref. 39).*

starch have been normalised to amylopectin from the relative areas under the $g^*(s)$ peaks. From this data a value for M_w of $\sim30\times10^6$ g mol^{-1} has been estimated.[39]

Equation (8) is only approximate – any contributions from molecular charge to the concentration dependence parameter k_s are assumed to be negligible or suppressed – but is nonetheless useful when other methods, especially for very large polysaccharides like amylopectin, are inapplicable. The method also provides an estimate for the swollen specific volume v_s: for example, Majzoobi has obtained a value of 40 ± 4 mL g^{-1} for wheat starch amylopectin.[39] For polydisperse materials such as polysaccharides, the question is what sort of average M value is yielded by doing so? In the absence of any obvious analytical solution, computer simulation has been used to determine the form of the average. In their work to be published, Rowe and co-workers have shown that even for 'unfavourable' simulated mixtures (*e.g.* multi-modal, no central tendency), the average M value yielded is very close to an M_w (*i.e.* weight-averaged M). To put this in quantitative terms, the departure from M_w is generally $<1\%$ of the way towards M_z. This is trivial, in terms of the errors present in the raw data. Thus, there is an exact procedure which can be defined for the evaluation of M(average) in a polydisperse solute system under the defined conditions, and simulation demonstrates that for all practical purposes the outcome is an M_w.

A sedimentation coefficient *distribution*, either $c(s)$ *vs.* s or $g^*(s)$ *vs.* s, for a polysaccharide can also be converted into an apparent molecular weight distribution if the conformation of the polysaccharide is known or can be assumed, via a power law or 'scaling' relation (see below). An early example of this transformation, assuming a random coil conformation, has been given for a heavily glycosylated mucin glycoprotein with polysaccharide-like properties[42] based on a $g^*(s)$ *vs.* s distribution given by Pain.[43] The assumption was made that the contribution from diffusion broadening of these large molecules was negligible in comparison to sedimentation.

4 Polysaccharide Molecular Weight Analysis by Sedimentation Equilibrium: MSTAR

The final steady-state pattern from a sedimentation equilibrium experiment[44] is a function only of molecular weight and related parameters (non-ideal virial coefficients and

association constants were appropriate) and not on molecular shape since at equilibrium there is no net transport or frictional effects: sedimentation equilibrium in the analytical ultracentrifuge provides an absolute way of estimating molecular weight. Since polysaccharides are by their very nature polydisperse, the value obtained will be an average of some sort. With Rayleigh interference and, where appropriate, UV-absorption optics, the principal average obtained is the weight average, M_w.[12] Although relations are available for also obtaining number-average M_n and z-average M_z data, these latter averages are difficult to obtain with any reliable precision. Direct recording of the concentration gradient dc/dr *vs.* radial displacement r using refractive index gradient or 'Schlieren' optics however facilitates the measurement of M_z (see ref. 45). Although present on the older generation Model E and MOM centrifuges, Schlieren optics are not on the present generation XL-A or XL-I ultracentrifuges, except for in-house adapted preparative XL ultracentrifuges.[46]

An important consideration with polysaccharides is that at sedimentation equilibrium there will be a redistribution not only of total concentration of polysaccharide throughout the cell (low concentration at the meniscus building up to a higher concentration at the cell base) but also a redistribution of species of different molecular weight, with a greater proportion of the higher molecular-weight part of the distribution appearing near the cell base. In obtaining a true weight (or number, z averages), it is therefore important to consider the *complete* concentration distribution profile throughout the ultracentrifuge cell. As with our description of sedimentation velocity, for clarity, we will confine our consideration only to the extraction of the two most directly related parameters: the weight average molecular weight and the molecular weight distribution. The extraction of other parameters, such as point average data, are avoided here but can be found in other articles (see refs. 47–49).

4.1 Obtaining the Weight Average Molecular Weight

As stated above, UV-absorption optics, when they can be applied, have the advantage that the recorded absorbances $A(r)$ as a function of radial position are (within the Lambert–Beer law limit of $A(r)\sim1.4$) directly proportional to the weight concentration $c(r)$ in g mL^{-1}. Although the multiple fringes in interference optics give a much more precise record of concentration, we stress again, these are *concentrations relative to the meniscus, i.e.* we obtain directly from the optical records a profile of $c(r)-c(a)$ *vs.* radial displacement r, with the meniscus at $r=a$. In fringe displacement units, this is $J(r)-J(a)$, which we write as $j(r)$ for short. To obtain molecular weight information, we need $J(r)$ and hence, some way of obtaining $J(a)$ is required: this is not such a requirement for sedimentation velocity where relative concentrations are sufficient. Any attempt to deplete the meniscus (rich in the lower molecular-weight part of the distribution) of a polysaccharide solution so that $J(a)\sim0$ – a method popular for protein work since 1964[50] – is almost guaranteed to result in loss of optical registration of the interference fringes near the bottom of the cell, leading to underestimates for M_w. This means that a procedure for evaluating $J(a)$ is required. It was recently shown by Hall and co-workers[51] that simply floating it as another variable in the procedure for extracting M is not valid, particularly for polydisperse or interacting systems. A convenient procedure for extracting $J(a)$ and then

M_w was given by Creeth and Harding in 1982:[52] the fundamental equation of sedimentation equilibrium can be manipulated to define a new function with dimensions of molar mass (g mol^{-1}) called $M^*(r)$. $M^*(r)$ at a radial position r is defined by

$$M^*(r) = j(r)/\{kJ(a)(r^2-a^2) + 2k\int_a^r rj(r)\,dr\} \tag{9}$$

where $k = (1-\bar{v}\rho_o)\omega^2/2RT$, with ρ_o the solvent density. Equation (9) has the limiting form

$$\lim_{r\to a}\left\{\frac{j(r)}{(r^2-a^2)}\right\} = kM^*(a)J(a) \tag{10}$$

A plot of $j(r)/(r^2-a^2)$ *vs.* $\{1/(r^2-a^2)\}\int_a^r rj(r)\,dr$ therefore has a limiting slope of $2kM^*(a)$ and an intercept $kM^*(a)J(a)$. Hence $J(a)$ is determinable from 2× (intercept/limiting slope). Other methods of obtaining $J(a)$ have been considered in detail by Teller and co-workers[53] and Creeth and Pain.[47] More recently, Minton[54] has given an almost identical procedure, although unfortunately he appears to have missed the original Creeth and Harding article published 12 years earlier.[52] Once $J(a)$ has been found, M^* as a function of radial position r can be defined. A particularly useful property of the M^* function is that at the cell base ($r=b$),

$$M^*(b) = M_{w,app} \tag{11}$$

the apparent weight average molecular weight of the polysaccharide.[52] It will be an 'apparent' value because it will be affected by thermodynamic non-ideality (molecular co-exclusion and, for charged polysaccharides, polyelectrolyte behaviour), which needs to be corrected for (see below). Optical distortion effects at the cell base means that a short extrapolation of $M^*(r)$ to $M^*(=b)$ is required, but this normally poses no difficulty. Practical details behind the MSTAR algorithm upon which this procedure is based can be found in refs. 48, 49 and 55. It is worth pointing out here that another popular algorithm for analysing molecular weight from sedimentation equilibrium is NONLIN.[56] Whereas this is useful for the analysis of protein systems (monodisperse or associating), for polydisperse system like polysaccharides, it is unsuitable: the estimate for $M_{w,app}$ obtained refers only to a selected region of the ultracentrifuge cell, and provides no rigorous procedure for dealing with the meniscus concentration problem.

4.2 Correcting for Thermodynamic Non-Ideality: Obtaining M_w from $M_{w,app}$

For polysaccharides, non-ideality arising from co-exclusion and polyelectrolyte effects can be a serious problem and, if not corrected for, can lead to significant underestimates for M_w. It was possible with the older generation Model E ultracentrifuges, which could accommodate long (30 mm) optical path length cells to work at very low solute loading concentrations (0.2 mg mL^{-1}). At these concentrations, for some polysaccharides, the non-ideality effect could be neglected: the estimate for $M_{w,app}$ was within a few percent of the true or 'ideal' M_w. However, the new-generation XL-I can

only accommodate a maximum 12 mm optical path length cell with a minimum concentration requirement of 0.5 mg mL^{-1}: lower concentrations produce insufficient fringe displacement for meaningful analysis. This makes a large difference to the severity of the non-ideality problem: a concentration extrapolation is now mandatory for sedimentation equilibrium molecular weight determinations on polysaccharides using an equation of the form[47]

$$\{1/M_{w,app}\} = \{1/M_w\} + 2Bc \qquad (12)$$

$$= \{1/M_w\}(1 + 2BM_wc)$$

correct to first order in concentration. In connection with this correction, it is worth mentioning (1) The availability of four- and eight-hole rotors in the XL-A and XL-I means that several concentrations can be run simultaneously. Further multiplexing is possible with the use of style six-channnel ultracentrifuge cells,[50] which permit the simultaneous measurement of three solution/reference solvent pairs, although these tend to return $M_{w,app}$ values of lower accuracy. (2) For polyelectrolytes, the second virial coefficient is very sensitive to ionic strength. Preston and Wik[4] have shown a 10-fold increase in B, from ~50 to ~500 mL mol g^{-2}, upon decreasing the ionic strength from 0.2 down to 0.01 mol L^{-1}. (3) The second virial coefficient B in Equation (12) refers to the static case. In the ultracentrifuge, the measured value can show a speed dependence,[57] an effect which can be minimized by using low speeds and short solution columns. If present, it will not affect the value of M_w after extrapolation to zero concentration. (4) In some extreme cases, third or even higher virial coefficient(s) may be necessary to adequately represent the data, for example, κ-carrageenan[58] and alginate.[59] In a further study on alginates, Straatman and Borchard[60] demonstrated excellent agreement between M_w and B values obtained from sedimentation equilibrium and light-scattering methods.

4.3 Distributions of Molecular Weight: SEC–MALLs and the New Role for Sedimentation Equilibrium

Direct inversions of the concentration distribution profiles to obtain molecular weight distribution information are generally intractable because of complications involving non-ideality. Successful attempts have been given but only for simple discrete forms of polydispersity (two to three macromolecular species.[61] The simplest procedure for avoiding these complications[62] is to use sedimentation equilibrium in conjunction with gel-permeation chromatography (GPC). Fractions of relatively narrow (elution volume) bandwidth are isolated from the eluate and their M_w values evaluated by low-speed sedimentation equilibrium in the usual way: the GPC columns can thereby be 'self-calibrated' and elution volume values converted into corresponding molecular weights – a distribution can therefore be defined in a way which avoids the problem of using inappropriate standards for GPC: the value of multiplexing is clearly indicated. This procedure has been successfully applied, for example, to dextrans, alginates and pectins: for pectins, excellent agreement with analogous procedures involving classical light scattering coupled to GPC has been obtained.[63]

There is now a much easier method available for obtaining molecular weight distribution. The measurement of the angular dependence of the total intensity of light scattered by solutions of polysaccharides provides, like sedimentation equilibrium, a direct and absolute way of measuring the weight average molecular weight, again if allowance for thermodynamic non-ideality is made. (Some researchers tend to prefer 'A_2' as notation for the second virial coefficient rather than B.) Although opinions varied, prior to 1990 (see *e.g.* ref. 64), there was good case for suggesting sedimentation equilibrium as the preferred method of choice for the measurement of molecular weights, simply because of the less stringent requirements on sample clarity: with light scattering, it is essential that solutions are free of supra-molecular aggregates. The inclusion of a flow cell into a light-scattering photometer facilitated the coupling on-line to a gel-permeation chromatography column and SEC–MALLs has now revolutionised the measurement of molecular weight and molecular weight distribution.[65,66] The combined effect of the SEC columns and a pre- or 'guard column' can provide clear fractionated samples to the light-scattering cell, facilitating not only measurement of M_w for the whole distribution, but also the distribution itself. Prior ultracentrifugation of the polysaccharide solution (~40 000 rpm for 30 min) is still advisable. The first polysaccharides studies were published in 1991[67–69] and it is now regarded by many as the method of choice for polysaccharide molecular weight determination. Furthermore, the angular dependence of the scattered light facilitates measurement of R_g as a function of elution volume and hence molecular weight: the method provides conformation information about the polysaccharide.[70] Nonetheless uncertainties can sometimes remain, particularly if materials have been incompletely clarified or there are problems with the columns (the form of the angular dependence data can usually tell us if things are not well). Sedimentation equilibrium offers a powerful and valuable independent check on the results generated from SEC–MALLs: although it takes a longer time to generate a result, and molecular weight distributions are considerably more difficult to obtain, agreement of M_w from sedimentation equilibrium with M_w from SEC–MALLs gives the researcher increased confidence in some of the other information (molecular weight distribution and R_g–M dependence) coming from the latter.

5 Polysaccharide Conformation Analysis by Sedimentation Velocity

The sedimentation coefficient s^o provides a useful indicator of polysaccharide conformation and flexibility in solution, particularly if the dependence of s^o on M_w is known.[41] There are two levels of approach: (i) a 'general' level in which we are delineating between overall conformation types (coil, rod, sphere), (ii) a more detailed representation where we are trying to specify particle dimensions in the case of rigid structures or persistence lengths for linear, flexible structures.

5.1 The Wales–van Holde Ratio

The simplest indicator of conformation comes not from s^o but the sedimentation concentration dependence coefficient, k_s. Wales and van Holde[71] were the first to show

that the ratio of k_s to the intrinsic viscosity $[\eta]$ was a measure of particle conformation. It was shown empirically by Creeth and Knight[72] that this ratio has a value of ~1.6 for compact spheres and non-draining coils, and adopted lower values for more extended structures. Rowe[16,17] subsequently provided a derivation for rigid particles, a derivation later supported by Lavrenko and co-workers.[2] The Rowe theory assumed there were no free-draining effects and also that the solvent had sufficient ionic strength to suppress any polyelectrolyte effects. A value of 1.6 was evaluated for spheres, reducing to ~0.2 for long rod-shaped molecules.

Lavrenko and co-workers[2] also examined in detail the effects of free draining of solvent during macromolecular motion, demonstrating that this also had the effect of lowering $k_s/[\eta]$. A hydrodynamic intra-chain interaction or 'draining' parameter has been defined[73] with limits $X=\infty$ for the non-free draining case and $X=0$ for the free-draining case. A relation was given between $k_s/[\eta]$ and X:[2,73]

$$\{k_s/[\eta]\} = \frac{8X}{(3 + 8X)} \tag{13}$$

This relation evidently leads to theoretical limits for $k_s/[\eta]=0$ for free draining and 1 for non-free draining. The consequences of this are that unless the draining characteristics of the chain are properly known, one has to be cautious in making conclusions about particle asymmetry, since it has been claimed that draining affects can mimic increase in asymmetry in lowering the $k_s/[\eta]$. Notwithstanding, many non-spherical molecules have empirical values for $k_s/[\eta] > 1.0$: pullulans,for example, considered as a random coil have been shown to have $k_s/[\eta] \sim 1.4$ (see ref. 74). Berth and co-workers[75] have argued that the very low $k_s/[\eta]$ values for chitosans are due to draining effects rather than a high degree of extension. Lavrenko and co-workers[2] have compiled an extensive list of $k_s/[\eta]$ values for a large number of other polysaccharides, complementing a list given by Creeth and Knight:[72] values are seen to range from 0.1 (potato amylose in 0.33 M KCl) to 1.8 (a cellulose phenylcarbamate in 1,4 dioxane), with some polysaccharides showing a clear dependence on molecular weight.

5.2 Power Law or 'Scaling' Relations

The relation linking the sedimentation coefficient with the molecular weight for a homologous polymer series given above is (see refs. 40 and 76):

$$s = K''M^b \tag{14}$$

(Some researchers (see *e.g.* ref. 2) call the exponent $1-b$.) This relation is similar to the well-known Mark–Houwink–Kuhn–Sakurada relation linking the intrinsic viscosity with molecular weight:

$$[\eta] = K'M^a \tag{15}$$

and also a relation linking the radius of gyration R_g with molecular weight:

$$R_g = K''M^c \tag{16}$$

Table 1 *Power law exponents (from ref. 40)*

	a	*b*	*c*
Sphere	0	0.67	0.33
Coil	0.5–0.8	0.4–0.5	0.5–0.6
Rod	1.8	0.15	1.0

The power law or 'MHKS' exponents *a*,*b*,*c* have been related to conformation[40,41] (Table 1).

The coefficients in Table 1 correspond to the non-draining case. If draining effects are present then these will change the values for *a* and *b* (see *e.g.* ref. 77). For example, it has been shown that *a* varies from 0.5 (non-draining case) to 1 (draining), again mimicking the effects of chain elongation.

Another scaling relation exists between the sedimentation coefficient and k_s (see ref. 2):

$$k_s = K''''(s^o)^{\kappa} \tag{17}$$

and values of κ and K''' have been given for a range of polysaccharides.[2]

Various relations have been proposed linking the various power-law exponents for a homologous series under specified conditions[41] such as

$$\kappa = \frac{(2 - 3b)}{b} \tag{18}$$

5.3 General Conformation: Haug Triangle and Conformation Zoning

Delineation of the three general conformation extremes (random coil, compact sphere, rigid rod) as indicated by the simple power or scaling laws and Wales/van Holde ratio, have been conveniently represented in the well-known Haug triangle (see ref. 40). An extension of this idea was given by Pavlov and co-workers,[78,79] who suggested five general conformation types or 'zones', all of which could be distinguished using sedimentation measurements. The zones were: A (extra rigid rod), B (almost rigid rod), C (semi-flexible coil), D (random coil) and E (globular/branched). A and B are distinguished by B having a very limited amount of flexibility. The zones were constructed empirically using a large amount of data (s, k_s) accumulated for polysaccharides of 'known' conformation type, and plotted a scaling relation normalised with mass per unit length (M_L) measurements (Figure 3). The latter parameter can be obtained from knowledge of molecular weight from sedimentation equilibrium or light scattering and the chain length L from small-angle X-ray scattering, X-ray fibre diffraction or NMR. Pavlov and co-workers give a comprehensive comparison of methods for heparin.[36] If the molecular weight is known, M_L can also be estimated from electron microscopy.[80] Measurement of a data set (s, k_s, M_L) of any target polysaccharide would then establish its conformation type. The limiting slopes of ~4 (extra rigid rod) and ~0 (globular/sphere) were shown to be theoretically reasonable. Other normalised scaling relations have been suggested based on viscometry methods.[79]

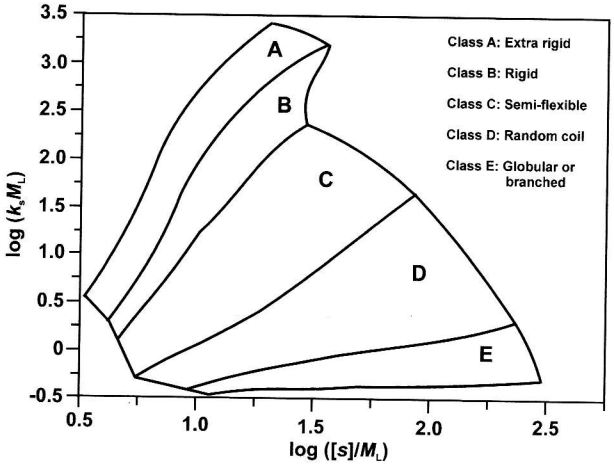

Figure 3 *Conformation zoning of polysaccharides. Empirical plots for various polysaccharides of known conformation type. This helps to define zones: (A) extra rigid rod, (B): rigid rod, (C) semi-flexible coil, (D) random coil, (E) globular/heavily branched structure. Measurement of s, k_s and M_L for a target polysaccharide then define its conformation zone or type (redrawn and based on ref. 78)*

5.4 Rigid Cylindrical Structures

Once a general conformation type or 'preliminary classification' has been established, it is possible to use sedimentation data to obtain more detailed information about polysaccharide conformation. For example, the low value of $k_s/[\eta]$ ~0.25 found for the bacterial polysaccharide xylinan has been considered to be due to asymmetry.[81] If we then assume a rigid structure, the approximate theory of Rowe[16,17] can be applied in terms of a prolate ellipsoid of revolution to estimate the aspect ratio p (~L/d for a rod, where L is the rod length and d its diameter) ~80.

For a cylindrical rod, an expression also exists for the sedimentation coefficient:[82]

$$s^o = \left\{\frac{M(1-\bar{v}\rho_o)}{(3\pi\eta_o N_A L)}\right\}\{\ln(L/d) + \gamma\} \tag{19}$$

where γ is a function of p and has a limiting value of ~0.386 for very long rods ($p \rightarrow \infty$). Replacing L by the (molar) mass per unit length $M_L = M/L$ (g mol^{-1} cm^{-1}), this becomes

$$s^o = \left\{\frac{M_L(1-\bar{v}\rho_o)}{(3\pi\eta_o N_A)}\right\}\{\ln M - \ln M_L - \ln d + \gamma\} \tag{20}$$

For the cases of finite p (in the range 2–20), the currently accepted expression for $\gamma(p)$ is that of Tirado and Garcia de la Torre:[83]

$$\gamma(p) = 0.312 + (0.561/p) + (0.100/p^2) \tag{21}$$

Above $p>10$, the limiting value (γ=0.386) can be used.

From Equations (20) and (21), we can obtain an estimate for the rod length L if we know M or M_L (see the above discussion) and have an estimate for the diameter d. As pointed out by Garcia de la Torre,[84] the choice for d is not so critical since it comes into the equations as the logarithm. It applies only to polysaccharides which are known to be rods.

5.5 Semi-Flexible Chains: Worm-Like Coils

Most linear polysaccharides are not rigid rods at all but are semi-flexible structures. The conformation and hydrodynamics of semi-flexible chains are most usefully represented by worm-like chains (see refs. 85–88), in which the bending flexibility is represented by the persistence length L_p. This is an intrinsic property of a linear macromolecule: the greater the L_p the greater the rigidity and *vice versa*. More precisely, the conformation and flexibility of a macromolecular chain depends directly on L/L_p, the ratio of the contour length to the persistence length. For $L/L_p \ll 1$ the conformation is rod-like and Equations (19)–(21) can be applied. For $L/L_p \gg 0$ the conformation approaches that of a random coil.[85–88] This can be best seen from the dependence of the radius of gyration on chain length, as clearly described by Freire and Garcia de la Torre:[88]

$$R_g^2 = \{L.L_p/3\}\{1 - (3L/L_p) + (6L_p^2/L^2) + 6(L_p^3/L^3)(1 - e^{-L/L_p})\} \qquad (22)$$

In the limit $L_p/L \sim 0$, R_g is proportional to $L^{1/2}$ (this is misprinted in ref. 88) – the classical dependence for a random coil – whereas when $L_p/L_o \gg 1$, the classical relation for a rod is obtained: $R_g = L/\sqrt{12}$.

The sedimentation coefficient for worm-like chains was first worked out by Hearst and Stockmayer,[89] later improved by Yamakawa and Fujii[90] to give this expression for s^o

$$s^o = \{M(1 - \bar{v}\rho_o)/(3\pi\eta_o N_A L)\}\{1.843 \ln\{L/2L_p)^{1/2} + \alpha_2 + \alpha_3(L/2L_p)^{-1/2} + \cdots\} \qquad (23)$$

If the persistence length L_p is much larger than the mean chain diameter d, Yamakawa and Fujii gave limiting values for $\alpha_2 = -\ln(d/2L_p)$ and $\alpha_3 = 0.1382$. Freire and Garcia de la Torre[88] have considered further these coefficients. The factor $2L_p$ appears rather than L_p simply because $2L_p$ is equivalent to the statistical Kuhn segment length λ^{-1}.

A fundamental problem with the sedimentation coefficient is that it is the least sensitive parameter to conformation when compared with the intrinsic viscosity $[\eta]$ and the radius of gyration R_g. This lower sensitivity is offset by the ease of measurement and the ability to obtain s^o to a higher accuracy (to better than 1%) compared with the other parameters. Nonetheless it is advisable not to use s in isolation but in conjunction with R_g and $[\eta]$ *vs.* M. Two recent examples are a comparative study using ultracentrifugation, viscometry and light scattering on the relative conformations and flexibilities of galactomannans (guar, tara gum and locust bean gum), after pressure-assisted solubilisation procedures[27] and a study using ultracentrifugation, viscometry and small-angle X-ray scattering to investigate the conformation and flexibility of heparin.[36]

6 Analysis of Polysaccharide Interactions

There are many instances where (associative) interactions involving polysaccharides, whether they be self-association, complex formation or with small ligands are important (see ref. 91). Examples of self-association are dimerisation or trimerisation of helical types of polysaccharides, such as schizophyllan, scleroglucan are good examples (we could mention also xanthan and κ-carrageenan although that has been the subject of some disagreement). Examples of complex formation include the use of cellulose derivatives as dental adhesives, and an example of small ligand interactions is the intercalation of iodine by amylose or amylopectin. There has been considerable attention focussed on the use of polysaccharide systems as encapsulation agents for flavours and drugs, and this invokes both macromolecular and small ligand interactions involving polysaccharides. The analytical ultracentrifuge would appear to offer considerable potential for the analysis of these and other types of interaction. Indeed one of the main reasons behind the renaissance of analytical ultracentrifugation in the 1990s[92,93] was the simmering need of molecular biologists and protein chemists for non-invasive solution-based methods for studying biomolecular interactions, particularly the weaker ones involved in molecular recognition phenomena (see *e.g.* refs. 94 and 95). The analytical ultracentrifuge – its clean, medium-free (no columns or membranes) and absolute nature has indeed proven a highly attractive tool for characterising the stoichiometry, reversibility and strength (as represented by the molar dissociation constant K_d) of an interaction between well-defined systems: protein–protein, protein–DNA, protein–small ligand. With polysaccharides, we are generally dealing with a different situation. Firstly, a polysaccharide does not have a single, clearly defined molecular weight: it is polydisperse with a distribution of molecular weights. Secondly, weak interactions (K_d>50 μM), at least as far as we know, do not play a crucial functional role with polysaccharides as they do with proteins. Interactions, particularly involving polyelectrolytes of opposite charge (chitosan–alginate for encapsulation systems, chitosan–DNA for gene therapy) tend to be very strong or irreversible: the complexes tend to be much larger than for the simple associative protein–protein interactions. This means the main ultracentrifuge tool used for investigating protein–protein interactions, namely sedimentation equilibrium, has only limited applicability: sedimentation equilibrium has an upper limit of molecular weight of ~50 million g mol^{-1}. Examples of the use of the analytical ultracentrifuge to assay interactions involving polysaccharides are a study on mixtures of alginate with bovine serum albumin,[96,97] a study of galactomannan incubated with gliadin (as part of an ongoing investigation into the possible use of galactomannans to help intestinal problems),[98] chitosan with lysozyme[99] and synergistic interactions involving xanthan.[100]

For large irreversible complexes involving polysaccharides, a more valid assay procedure is to use sedimentation velocity (which can cope with complexes as large as 10^9 g mol^{-1}), with change in sedimentation coefficient s (normalised to standard conditions or not) or as our marker for complex formation. If we so wish, we can then convert this to a change in molecular weight if we assume a conformation and use the power-law relation (Equation (13)). Alternatively, we can simply use s directly as our size criterion (this is not unusual; it is used, for example, in ribosome

size representations, 30S, 50S, ..., or in seed globulin, the 7S, 11S soya bean globulins, *etc.*[101]

A good example of where sedimentation velocity has played a valuable role in assaying large polysaccharide complexes is in the assessment of polysaccharides as mucoadhesives (see *e.g.* ref. 102 and references cited therein): a drug administered orally or nasally tends to be washed away from the site of maximum absorption by the body's natural clearance mechanisms before being absorbed. Incorporating the drug into a polysaccharide material which interacts with epithelial mucus in a controllable way has been proposed as a method of increasing the residence time and enhancing the absorption rate. The key macromolecule in mucus is mucin glycoprotein – a linear polypeptide backbone with linked saccharide chains to the extent >80% of the molecule is carbohydrate (see *e.g.* ref. 42). The carbohydrate has potential sites for ionic interaction (clusters of sialic acid or sulphate residues) and also hydrophobic interaction (clusters of methyl groups offered by fucose residues). The sedimentation ratio ($s_{complex}/s_{mucin}$) – the ratio of the sedimentation coefficient of the complex to that of the pure mucin itself – is used as the measure for effectiveness of a candidate mucoadhesive, supported by imaging (electron microscopy, scanning tunnelling microscopy and atomic force microscopy) and macroscopic studies. The UV absorption optics on the XL-A or XL-I ultracentrifuge have been used as the main optical detection system. Although the polysaccharide is generally invisible in the near UV (~280 nm), at the concentrations normally employed, the mucin, in uncomplexed and complexed form, is detectable. Experiments on a series of neutral and polyanionic polysaccharides revealed no significant change in the sedimentation coefficient (sedimentation ratio $s_{complex}/s_{mucin} \approx 1$) reinforcing macroscopic observations on whole mucus using tensiometry.[103] A contrasting picture is seen for polycationic deacetylated aqueous (pH<6) soluble derivatives of chitin known as chitosans with sedimentation coefficient ratios $s_{complex}/s_{mucin}$ approaching ~40. Interestingly, altering the degree of acetylation did not seem to affect the interaction greatly, suggesting that hydrophobic as well as electrostatic interactions play a mucoadhesive role. The demonstration of large-size interaction products by the analytical ultracentrifuge used in this manner is reinforced by images from the powerful imaging techniques of electron microscopy and atomic force microscopy. Conventional transmission electron microscopy clearly demonstrates large complexes of the order of ~1 μm in size,[104] and if we label the chitosan with gold we can see that the chitosan is distributed throughout the complex with 'hot spots' in the interior.[105] Images from atomic force microscopy, visualized in topographic and phase modes, again shows complexes of this size. Control experiments revealed a loose coiled structure for pig gastric mucin and a shorter, stiffer conformation for the chitosan, consistent with solution measurements.[106] The analytical ultracentrifuge procedure has also facilitated investigation of the effect of the solvent environment (pH, bile salts, *etc.*) on the extent of interaction.

6.1 Sedimentation Fingerprinting

A further modification of the procedure has been developed for the investigation of the interactions of human mucin from specific regions of the alimentary tract, generally extractable in only very small quantities, with chitosan. In this method, introduced in

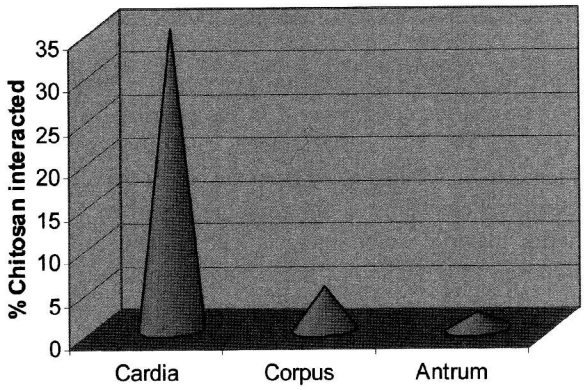

Figure 4 *Sedimentation fingerprinting analysis of the comparative mucoadhesiveness of a chitosan to mucins from different parts of the stomach (adapted from ref. 107)*

1999,[107] the Schlieren optical system is used to record the concentration (refractive index) gradient d*n*/d*r* as a function of radial position *r* in the ultracentrifuge cell. The area under a 'Schlieren peak' provides a measure of the sedimenting concentration. Alternatively, if interference optics on the XL-I ultracentrifuge are used, the area under a $g^*(s)$ *vs.* s or $c(s)$ *vs.* s plot would provide similar concentration information. Although the mucins from human stomach are at too low a concentration to be detected, we can assay for interaction from the loss of area under the chitosan peak caused by interaction. In this way, Deacon and co-workers[107] have shown it is possible to demonstrate significant differences in mucoadhesive interactions for different regions of the stomach (Figure 4).

This type of information obtained with the ultracentrifuge reinforced with other data is helping us design effective mucoadhesive systems. An example is the use of tripolyphosphate to cross-link chitosan into a sphere, and these have been shown to give good mucoadhesion.[108] If this is done in the presence of a drug, the drug can be encapsulated. Work is now in progress based around the principle of co-sedimentation[109] to investigate the encapsulation of drugs by these and similar delivery systems.

References

1. S. E. Harding, in *Analytical Ultracentrifugation in Biochemistry and Polymer Science*, S. E. Harding, A. J. Rowe and J. C. Horton (eds), Royal Society of Chemistry, Cambridge, UK, 1992, 495.
2. P. N. Lavrenko, K. J. Linow and E. Görnitz, in *Analytical Ultracentrifugation in Biochemistry and Polymer Science*, S. E. Harding, A. J. Rowe and J. C. Horton (eds), Royal Society of Chemistry, Cambridge, UK, 1992, 517.
3. W. D. Comper and O. Zamparo, in *Analytical Ultracentrifugation in Biochemistry and Polymer Science*, S. E. Harding, A. J. Rowe and J. C. Horton (eds), Royal Society of Chemistry, Cambridge, UK, 1992, 533.
4. B. N. Preston and K. O. Wik, in *Analytical Ultracentrifugation in Biochemistry and Polymer Science*, S. E. Harding, A. J. Rowe and J. C. Horton (eds), Royal Society of Chemistry, Cambridge, UK, 1992, 549.

5. S. E. Harding and A. J. Rowe, Opt. Laser. Eng., 1988, **8**, 83–96.
6. A. J. Rowe, S. Wynne-Jones, D. G. Thomas and S. E. Harding, in *Analytical Ultracentrifugation in Biochemistry and Polymer Science*, S. E. Harding, A. J. Rowe and J. C. Horton (eds), Royal Society of Chemistry, Cambridge, UK, 1992, 49–62.
7. A. J. Furst, *Eur. Biophys. J.*, 1997, **25**, 307.
8. R. Giebeler, in *Analytical Ultracentrifugation in Biochemistry and Polymer Science*, S. E. Harding, A. J. Rowe and J. C. Horton (eds), Royal Society of Chemistry, Cambridge, UK, 1992, 16.
9. H. Cölfen, S. E. Harding and K. M. Vårum, *Carbohyd. Polym.*, 1996, **30**, 5.
10. C. Theisen, C. Johann, M. P. Deacon and S. E. Harding, *Refractive Increment Data Book for Polymer and Biomolecular Scientists*, Nottingham University Press, Nottingham, UK, 2000.
11. M. W. Anthonsen, K. M. Vårum and O. Smidsrød, *Carbohyd. Polym.*, 1993, **22**, 193.
12. H. Schachman, *Ultracentrifugation in Biochemistry*, Academic Press, New York, 1959.
13. T. M. Laue, B. D. Shah, T. M. Ridgeway and S. L. Pelletier, in *Analytical Ultracentrifugation in Biochemistry and Polymer Science*, S. E. Harding, A. J. Rowe and J. C. Horton (eds), Royal Society of Chemistry, Cambridge, UK, 1992, 90.
14. http://www.jphilo.mailway.com/download.htm and http://www.rasmb.bbri.org/rasmb/windows/sednterp-philo/
15. N. Gralén, Sedmentation and diffusion measurements on cellulose and cellulose derivatives, Ph.D. Dissertation , University of Uppsala, Uppsala, Sweden, 1994.
16. A. J. Rowe, *Biopolymers*, 1977, **16**, 295.
17. A. J. Rowe, in *Analytical Ultracentrifugation in Biochemistry and Polymer Science*, S. E. Harding, A. J. Rowe and J. C. Horton (eds), Royal Society of Chemistry, Cambridge, UK, 1992, 394.
18. W. Stafford, in *Analytical Ultracentrifugation in Biochemistry and Polymer Science*, S. E. Harding, A. J. Rowe and J. C. Horton (eds), Royal Society of Chemistry, Cambridge, UK, 1992, 359.
19. J. S. Philo, *Anal. Biochem.*, 2000, **279**, 151.
20. P. Schuck, *Biophys. J.*, 1998, **75**, 1503.
21. J. Dam and P. Schuck, *Method. Enzymol.* 2003, **384**, 121.
22. http://www.jphilo.mailway.com/download.htm
23. O. Lamm, *Ark. Mat. Astr. Fys.*, 1923, **21B**(2), 1.
24. J. M. Claverie, H. Dreux and R. Cohen, *Biopolymers*, 1975, **14**, 1685.
25. http://www.analyticalultracentrifugation.com/download.htm
26. S. E. Harding, *Biophys. Chem.*, 1995, **55**, 69.
27. T. Patel, S. E. Harding, S. B. Ross-Murphy, D. R. Picout and G. Pavlov, 2005, in preparation.
28. T. Svedberg and K. O. Pedersen, *The Ultracentrifuge*, Oxford University Press, Oxford, UK, 1940.
29. E. V. Korneeva, G. A. Vichoreva, S. E. Harding and G. M. Pavlov, *Abstr. Am. Chem. Soc.*, 1996, **212**, 75.
30. G. M. Pavlov, E. V. Korneeva, S. E. Harding and G. A. Vichoreva, *Polymer*, 1998, **39**, 6951.
31. G. M. Pavlov, E. V. Korneeva, G. A. Vikhoreva and S. E. Harding, *Polym. Sci. Ser. A*, 1998, **40**, 1275 and *Vysokomolekulyarnye Soed. Ser. A.*, 1998, **40**, 2048.
32. G. M. Pavlov, E. V. Korneeva, S. A. Nepogod'ev, K. Jumel and S. E. Harding, *Polym. Sci. Ser. A*, 1998, **40**, 1282 and *Vysokomolekulyarnye Soed. Ser. A*, 1998, **40**, 2056.
33. G. M. Pavlov, E. V. Korneeva, K. Jumel, S. E. Harding, E. W. Meyer, H. W. I. Peerlings, J. F. Stoddart and S. A. Nepogodiev, *Carbohyd. Polym.* 1999, **38**, 195.
34. W. R. Sharman, E. L. Richards and G. N. Malcolm, *Biopolymers*, 1978, **17**, 2817.

35. D. J. Wedlock, B. A. Fasihuddin and G. O. Phillips, *Food Hydrocolloid.* 1987, **1**, 207.
36. G. Pavlov, S. Finet, K. Tatarenko, E. Korneeva and C. Ebel, *Eur. Biophys. J.*, 2003, **32**, 437.
37. W. Burchard, in *Laser Light Scattering in Biochemistry*, S. E. Harding, D. B. Sattelle and V. A. Bloomfield (eds), Royal Society of Chemistry, Cambridge, UK, 1992, 3.
38. P. N. Pusey, in *Photon Correlation and Light Beating Spectroscopy*, H. Z. Cummings and E. R. Pike (eds), Plenum Press, New York, 1974, 387.
39. M. Majzoobi, Ph.D. Dissertation, University of Nottingham, Nottingham, UK, 2004.
40. O. Smidsrød and I. L. Andresen, Biopolymerkjemi, Tapir, Trondheim, Norway, 1979.
41. V. N. Tsvetkov, V. Eskin and S. Frenkel, *Structure of Macromolecules in Solution*, Butterworths, London, 1970.
42. S. E. Harding, *Adv. Carbohyd. Chem.*, 1989, **47**, 345.
43. R. H. Pain, *Symp. Soc. Exp. Biol.*, 1980, **34**, 359.
44. T. Svedberg and R. Fåhraeus, *J. Am. Chem. Soc.*, 1926, **48**, 430.
45. A. C. Clewlow, N. Errington and A. J. Rowe, *Eur. Biophys. J.*, 1997, **25**, 305.
46. W. Mächtle, *Prog. Coll. Polym. Sci.*, 1999, **113**, 1.
47. J. M. Creeth and R. H. Pain, *Prog. Biophys. Mol. Biol.*, 1967, **17**, 217.
48. S. E. Harding, J. C. Horton and P. J. Morgan, in *Analytical Ultracentrifugation in Biochemistry and Polymer Science*, S. E. Harding, A. J. Rowe and J. C. Horton (eds), Royal Society of Chemistry, Cambridge, UK, 1992, 275.
49. H. Cölfen and S. E. Harding, *Eur. Biophys. J.*, 1997, **24**, 333.
50. D. A. Yphantis, *Biochemistry*, 1964, **3**, 297.
51. D. R. Hall, S. E. Harding and D. J. Winzor, *Prog. Coll. Polym. Sci.*, 1999, **113**, 62.
52. J. M. Creeth and S. E. Harding, *J. Biochem. Biophys. Meth.*, 1982, **7**, 25.
53. D. C. Teller, J. A. Horbett, E. G. Richards and H. K. Schachman, *Ann. New York Acad. Sci.*, 1969, **164**, 66.
54. A. P. Minton, in *Modern Analytical Ultracentrifugation*, T. M. Schuster and T. M. Laue (eds), Birkhäuser, Boston, 1994, 81.
55. http://www.nottingham.ac.uk/ncmh/unit/method.html#Software
56. http://www.biotech.uconn.edu/uaf
57. H. Fujita, *Foundations of Ultracentrifugal Analysis*, Wiley, New York, 1975.
58. S. E. Harding, K. Day, R. Dhami and P. M. Lowe, *Carbohyd. Polym.*, 1997, **32**, 81.
59. J. C. Horton, S. E. Harding, J. R. Mitchell and D. F. Morton-Holmes, *Food Hydrocolloid.*, 1991, **5**, 125.
60. A. Straatman and W. Borchard, *Prog. Coll. Polym. Sci.*, 2002, **119**, 64–69.
61. S. E. Harding, *Biophys. J.*, 1985, **47**, 247.
62. A. Ball, S. E. Harding and J. R. Mitchell, *Int. J. Biol. Macromol.*, 1988, **10**, 259.
63. S. E. Harding, G. Berth, A. Ball, J. R. Mitchell and J. Garcia de la Torre, *Carbohyd. Polym.*, 1991; **16**, 1.
64. S. E. Harding, *Gums Stablisers Food Ind.*, 1988, **4**, 15.
65. P. J. Wyatt, in *Laser Light Scattering in Biochemistry*, S. E. Harding, D. B. Sattelle and V. A. Bloomfield (eds), Royal Society of Chemistry, Cambridge, UK, 1992, 35.
66. http://www.wyatt.com/
67. J. C. Horton, S. E. Harding and J. R. Mitchell, *Biochem. Soc. Trans.*, 1991, **19**, 510.
68. J. E. Rollings, *Biochem. Soc. Trans.*, 1991, **19**, 493.
69. J. E. Rollings, in *Laser Light Scattering in Biochemistry*, S. E. Harding, D. B. Sattelle and V. A. Bloomfield (eds), Royal Society of Chemistry, Cambridge, UK, 1992, 275.
70. D. Wolff, S. Czapla, A. G. Heyer, S. Radosta, P. Mischnick and J. Springer, *Polymer*, 2000, **41**, 8009.
71. M. Wales and K. E. van Holde, *J. Polym. Sci.*, 1954, **14**, 81.

72. J. M. Creeth and C. G. Knight, *Biochim. Biophys. Acta*, 1965, **102**, 549.
73. K. F. Freed, *J. Chem. Phys.*, 1976, **65**, 4103.
74. K. Kawahara, K. Ohta, H. Miyamoto and S. Nakamura, *Carbohyd. Polym.*, 1984, **4**, 335.
75. G. Berth, H. Cölfen and H. Dautzenberg, *Progr. Colloid Polym. Sci.*, 2002, **119**, 50.
76. S. E. Harding, K. M. Vårum, B. T. Stokke and O. Smidsrød, *Adv. Carbohyd. Anal.*, 1991, **1**, 63.
77. G. M. Pavlov, *Progr. Colloid Polym. Sci.*, 2002, **119**, 84.
78. G. M. Pavlov, A. J. Rowe and S. E. Harding, *Trends Anal. Chem.*, 1997, **16**, 401.
79. G. M. Pavlov, S. E. Harding and A. J. Rowe, *Prog. Coll. Int. Sci.*, 1999, **113**, 76.
80. B. T. Stokke and A. Elgsaeter, *Adv. Carbohyd. Anal.*, 1991, **1**, 195.
81. S. E. Harding, G. Berth, J. Hartmann, K. Jumel, H. Cölfen, B. E. Christensen, *Biopolymers*, 1996, **39**, 729.
82. S. Broesma, *J. Chem. Phys.*, 1960, **32**, 1626.
83. M. M. Tirado and J. Garcia de la Torre, *J. Chem. Phys.*, 1979, **71**, 2581.
84. J. Garcia de la Torre, in *Analytical Ultracentrifugation in Biochemistry and Polymer Science*, S. E. Harding, A. J. Rowe and J. C. Horton (eds), Royal Society of Chemistry, Cambridge, UK, 1992, 333.
85. H. Yamakawa, *Modern Theory of Polymer Solutions*, Harper and Row, New York, 1971.
86. V. A. Bloomfield, D. M. Crothers and L. Tinoco, *Physical Chemistry of Nucleic Acids*, Harper and Row, New York, 1974.
87. C. R. Cantor and P. R. Schimmel, *Biophysical Chemistry*, Freeman, New York, 1979.
88. J. J. Freire and J. Garcia de la Torre, in *Analytical Ultracentrifugation in Biochemistry and Polymer Science*, S. E. Harding, A. J. Rowe and J.C Horton (eds), Royal Society of Chemistry, Cambridge, UK, 1992, 346.
89. J. E. Hearst and W. H. Stockmayer, *J. Chem. Phys.*, 1962, **37**, 1425.
90. H. Yamakawa and M. Fujii, *Macromolecules*, 1973, **6**, 407.
91. M. P. Tombs and S. E. Harding, *An Introduction to Polysaccharide Biotechnology*, Taylor and Francis, London, 1997.
92. H. K. Schachman, *Nature*, 1989, **941**, 259.
93. H. K. Schachman, in *Analytical Ultracentrifugation in Biochemistry and Polymer Science*, S. E. Harding, A. J. Rowe and J. C. Horton (eds), Royal Society of Chemistry, Cambridge, UK, 1992, 3.
94. J. D. Watson, *The Molecular Biology of the Gene*, 2nd edn, Benjamin, New York, 1970.
95. H. Silkowski, S. J. Davis, A. N. Barclay, A. J. Rowe, S. E. Harding and O. Byron, *Eur. Biophys. J.*, 1997, **25**, 455.
96. S. E. Harding, K. Jumel, R. Kelly, E. Gudo, J. C. Horton and J. R. Mitchell, in *Food Proteins: Structure and Functionality*, K. D. Schwenke and R. Mothes (eds), VCH Verlagsgesellschaft, Weinheim, Germany, 1993, 216.
97. R. Kelly, E. S. Gudo, J. R. Mitchell and S. E. Harding, *Carbohyd. Polym.*, 1994, **23**, 115.
98. A. Seifert, L. Heinevetter, H. Cölfen and S. E. Harding, *Carbohyd. Polym.*, 1995, **28**, 239.
99. H. Cölfen, S. E. Harding, K. M. Vårum and D. J. Winzor, *Carbohyd. Polym.*, 1996, **30**, 45.
100. R. O. Mannion, C. D. Melia, B. Launay, G. Cuvelier, S. E. Hill, S.E. Harding and J. R. Mitchell, *Carbohyd. Polym.* 1992, **19**, 91.
101. K. D. Schwenke, *Eiweißquellen der Zukunft*, Urania-Verlag, Leipzig, German Democratic Republic, 1985.
102. S.E. Harding, *Biochem. Soc. Trans.*, 2003, **31**, 1036.
103. C. M. Lehr, J. A. Bouwstra, E. H. Schacht and H. E. Junginger, *Int. J. Pharmaceut.*, 1992, **78**, 43.
104. I. Fiebrig, S. E. Harding, A. J. Rowe, S. C. Hyman and S. S. Davis, *Carbohyd. Polym.*, 1995, **28**, 239.

105. I. Fiebrig, K. M. Vårum, S. E. Harding, S. S. Davis and B. T. Stokke, *Carbohyd. Polym.*, 1997, **33**, 91.
106. M. P. Deacon, S. McGurk, C. J. Roberts, P. M. Williams, S. J. B. Tendler, M. C. Davies, S. S. Davis and S. E. Harding, *Biochem. J.*, 2000, **348**, 557.
107. M. P. Deacon, S. S. Davis, R. J. White, H. Nordman, I. Carlstedt, N. Errington, A. J. Rowe and S. E. Harding, *Carbohyd. Polym.*, 1999, **38**, 235.
108. P. He, S. S. Davis and L. Illum, *Int. J. Pharm.*, 1998, **166**, 75.
109. S. E. Harding and D. J. Winzor, in *Protein–Ligand Interactions: Hydrodynamics and Calorimetry*, S. E. Harding and B. Z. Chowdhry (eds), Oxford University Press, Oxford, 2001, 75–103.